2014 IEEE International Conference on Robotics & Automation (ICRA)
Hong Kong Convention and Exhibition Center
May 31 - June 7, 2014. Hong Kong, China

On the Analysis of Large-Dimension Reconfigurable Suspended Cable-Driven Parallel Robots

Dinh Quan Nguyen, Marc Gouttefarde, Olivier Company and François Pierrot *

***Abstract*— In this paper, a new type of large-dimension reconfigurable suspended cable-driven parallel robots (CDPR) is introduced as a means to substitute for conventional methods of handing large and heavy parts across wide workspaces. The reconfigurability of the proposed CDPR offers better performances in term of workspace, flexibility and power consumption. A systematic procedure to solve a complex nonlinear optimization problem to find optimal reconfiguration for the robot is presented. Critical issues regarding various constraints and performance criteria are addressed. The robot can operate in offline reconfiguration or online reconfiguration modes which offer wide range of solutions to the end-users.**

I. INTRODUCTION

In the past twenty years, cable-driven parallel robots have been extensively studied in favor of their appealing advantages, compared to parallel manipulators with rigid links, such as: light weight, large workspace, high load capacity, ease of construction, ease of reconfiguration and low cost.

Possible applications of CDPR in the manufacturing, construction and aerospace industries are positioning and handling of large and heavy parts across wide workspaces. For example, Fig. 1 shows a conventional method to handle large and heavy parts in a workshop by using multiple cranes to manipulate the parts. This solution has several limits including limited flexibility and orientation capabilities. Most of the time when the operation requires a change of orientation of the part, there is a need of involving workers which causes safety issues. Another example in the aerospace industry is the airplane maintenance operations which is illustrated in Fig. 2 where the workers are performing painting tasks[1]. Several telescopic platforms are used to carry the workers across the airplane fuselage. Each telescopic platform offers 4 degrees of freedom (three translations in Cartesian space and one rotation around the vertical z-axis) which allows the task to be done quite efficiently. However, this solution has some disadvantages. First of all, each telescopic platform weights from 9 to 11 tons which implies high costs for the building construction to sustain such heavy systems. Furthermore, the workers sometimes need to work in hazardous environment where the operation requires to use chemical material like paint or stripping products. Our motivations in this paper comes directly from the need of looking for alternative solutions in such situations to replace conventional methods. By using large-dimension reconfigurable CDPR we could reduce the cost of construction and improve the flexibility as well as the capacity of the systems and offer a wider range of applications to the end-users.

Most of the past research efforts focused mainly on conventional CDPR with winches and cable exits points fixed at given locations in the base frame. Among them, several studies on large-dimension CDPR have been made [1]–[14]. Notable CDPR prototypes which can handle heavy payloads are the early NIST RoboCrane [1], the large-dimension CDPR in FAST project [8]–[10], the Marionet crane robot [15] and CoGiRo [16]. In [17], a solution using cable robots to handle heavy parts in airplane maintenance has been implemented. The introduced AMP cable robot uses NISTs RoboCrane technology in which six hoist cables from three upper support points tautly support, stabilize, and maneuver the work platform. To our best knowledge, there is no published technical paper about the AMP.

* Dinh Quan Nguyen, Marc Gouttefarde, Olivier Company and François Pierrot are with the Laboratoire d'Informatique, de Robotique et de Microélectronique de Montpellier (LIRMM-CNRS-UM2), 161 rue Ada, 34392 Montpellier Cedex 5, France dinhquan.nguyen@lirmm.fr, marc.gouttefarde@lirmm.fr, company@lirmm.fr, pierrot@lirmm.fr

[1] https://blog.klm.com/not-just-any-paint-job/1533/

Fig. 1: Handling heavy parts using cranes

Fig. 2: Airplane maintenance workshop

Recent studies [15], [18]–[20] deal with reconfigurable CDPR where the geometry structure of the CDPR can be reconfigured by changing its cable layout. Such reconfigurability could greatly increase the CDPR capability. Meanwhile, it adds redundancy and increases the complexity of the system. For the design of such CDPR, in [18], Rosati introduced the concept of adaptive cable-driven systems. He discussed a systematic procedure to determine the design solution for planar cable-driven systems which minimizes or maximizes some local performance indices such as cable tension based criteria and dexterity of the CDPR. Later on, Xiaobo Zhou in [19] presented an analysis framework for cooperating cable mobile robots. The proposed method to solve the reconfiguration of such systems is similar to that of Rosati in the sense that the solutions were derived from optimizing certain criteria. In [20], Zhou et al. proposed a generalized modeling framework for systematic design and analysis of cooperative mobile cable robots. They deal with the redundancy resolution by optimally repositioning the mobile bases to maximize the so-called tension factor which is the ratio between minimal and maximal values of cable tensions along a given trajectory. However, all these previous studies only consider planar robot systems where important constraints such as cable interferences are not taken into account. Moreover, critical issues while using standard optimization tools to solve the redundancy of the robot system such as:

- the continuity of the performance indices with respect to the deciding parameters
- the continuity and differentiability of the constraints

have not been addressed. In fact, the continuity of the tension based performance indices can be dealt with by using tension distribution method such as the one in [21]. However, it is difficult to address the second issue since there are different types of constraints including wrench feasibility (continuous nonlinear constraints) and cable interferences (non-differentiable constraints). Furthermore, the problem becomes more complex for a highly redundant CDPR. Because of these issues, the implementation of the existing methods in solving the reconfiguration of a 6-DOF CDPR is an issue, especially under real-time constraints.

The contributions of the present paper are mainly focused on the use of gradient-based optimization tools to solve the CDPR reconfiguration. First, we introduce a particular type of large-dimension reconfigurable suspended CDPR which offers alternative solutions to the conventional methods of handling large and heavy parts across wide workspaces. Then, a systematic procedure to solve the reconfiguration of such systems is proposed. The CDPR reconfiguration is divided into two sub-optimization problems. The first problem consists of finding the bounds on the reconfiguration parameters in which all the nonlinear constraints including wrench feasibility and geometric constraints are satisfied. The CDPR reconfiguration is thereby transformed into a classical box-constrained problem which can be solved with standard optimization tools. Two reconfiguration strategies are considered: *offline reconfiguration* and *online reconfiguration*. Two criteria are introduced to quantify the robot performance in term of power consumption: *the sum of cable tensions* (used in offline reconfiguration) and *minimal energy consumption of the CDPR* (used in online reconfiguration). The procedure provides a straightforward approach which is familiar to engineers and could be implemented in real-time software environments.

The paper is organized as follows. Section II presents the general architecture of the new type of reconfigurable CDPR considered in this paper. Section III recalls the usual modeling of CDPR. The procedure to solve the reconfiguration is discussed in Section IV. Simulation examples are presented in Section V. Finally, some remarks on our proposed methodology are made in Section VI.

II. LARGE-DIMENSION RECONFIGURABLE CDPR ARCHITECTURE

Fig. 3 shows the general concept of large-dimension reconfigurable suspended CDPR considered in this paper to replace conventional cranes or telescopic platforms as those shown in Fig. 1 and Fig. 2. The winches that drive the cables are attached onto two overhead bridge cranes to form a large-dimension CDPR. The positions of the winches or cable exit points can be changed by mobile bases that ride on each crane. The overhead bridge cranes can move along the side walls of the workshop building. In this way, each CDPR should cover any area in the workshop. Depending on the size of the workshop, multiple CDPR can be used to perform different tasks across wide workspaces.

In fact, this idea is derived originally from the experiences of partners involved in the CableBOT[2] consortium. Firstly, the general suspended architecture of the reconfigurable CDPR is similar to that of the fixed-configuration redundant suspended CDPR CoGiRo prototype [16] since CoGiRo's geometry structure has shown some great potential. Secondly, the moving cranes are adapted from the overhead bridge crane systems that carry heavy parts in workshops.

[2]http://www.cablebot.eu

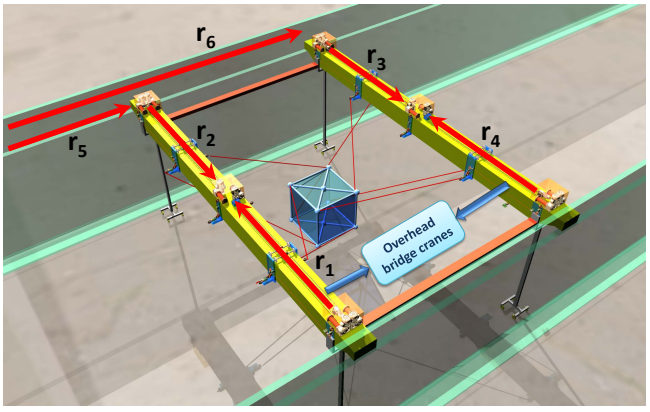

Fig. 3: Solution using large-dimension reconfigurable suspended CDPR to replace conventional cranes

By attaching the winches on the cranes, there will be mostly vertical forces acting on the two side walls of the building. Lateral force components created by cables tensions which are orthogonal to the side walls are minimized. However, horizontal force components in the cables that tend to bring the two overhead bridge cranes together may need to be avoided. One solution is to connect the two cranes with some support beams to sustain these horizontal forces. In this manner, the robot system loses one degree of redundancy but, in return, becomes more stable.

In the general scenario, the 6-DOF mobile platform of the CDPR is driven by 8 cables and two overhead bridge cranes. Each cable exit point is driven by an actuator. If all the cable exit points could move freely along the bridge cranes, the number of total actuators would be 18 (here, 10 actuators are used to reconfigure the robot geometry structure). It results in a highly redundant robot system. We propose to move the cable exit points by pairs along the bridges to reduce the total number of actuator from 18 to 14. If we fix the cable exit points and also the positions of two overhead bridge cranes, the total number of actuators that drive the mobile platform is reduced to 8. In this latter case, the CDPR becomes one similar to the fixed-configuration redundant CDPR (e.g. CoGiRo prototype).

In the most complex case considered in this paper, the reconfigurability of the proposed CDPR is determined by a maximum of 6 actuators that drive the 4 pairs of cable exit points $(r_1, ..., r_4)$ and the 2 overhead bridge cranes (r_5, r_6), as shown in Fig. 3. Hence, $(r_1, r_2, ..., r_6)$ are the reconfiguration parameters. Note that the positions of the two overhead bridge cranes can be fixed in order for the CDPR to perform at specific areas in the workshop. In such cases, there are only four reconfiguration parameters r_1, r_2, r_3 and r_4.

It is worth noting that, by keeping the general suspended redundant structure similar to the CoGiRo prototype [21] (using 8 cables to drive the mobile platform), the Cartesian workspace and orientation workspace of the CDPR are increased substantially, compared to 6-cable CDPR such as the AMP [17]. Furthermore, reconfigurability should improve the CDPR performances and offers more flexible choices to the end-users (in the present paper, *reconfigurability* means the ability to change the locations of the cable exit points of the CDPR).

The CDPR can operate in two modes, *offline reconfiguration* and *online reconfiguration*. In *offline reconfiguration*, appropriate positions of the cable exit points are determined offline. Thereby, the geometric structure of the CDPR is adapted to the tasks at hand. After the reconfiguration of cable exit points has been performed, the cable exit point positions are fixed and the robot starts the given tasks. Meanwhile, *online reconfiguration* consists in changing the positions of the cable exit points along a trajectory followed by the CDPR mobile platform.

III. MODELING

Fig. 4 shows the general structure of a CDPR which includes *the cable and winches* driving the mobile platform, *the cable exit points* A_i, *the cable anchor points* B_i and the *mobile platform*. By controlling the length of each cable, a CDPR can directly position its end-effector.

A. Solving the cable tension distribution of a CDPR

For large-dimension CDPR handling heavy payloads (could be over 1 ton), hefty steel cables are used because of high safety factors. The sagging of cables may affect the robot performances [11]–[13]. Cable models with non-negligible mass and elasticity must be taken into account. By using the simplified cable model derived in [13], [14], one can solve the tension distribution problem of a CDPR with hefty steel cables using efficient methods such as the one in [21]. The cable tensions satisfy the equilibrium equations of the mobile platform (1):

$$\mathbf{W}\,\boldsymbol{\tau}_b = \mathbf{f_e} \tag{1}$$

subject to

$$\tau_{\min} \le \tau_{bi} \le \tau_{\max} \left(i = \overline{1, m}\right) \tag{2}$$

where

$$\mathbf{W} = \begin{bmatrix} \mathbf{u}_1 & \mathbf{u}_2 & \cdots & \mathbf{u}_m \\ \mathbf{b}_1 \times \mathbf{u}_1 & \mathbf{b}_2 \times \mathbf{u}_2 & \cdots & \mathbf{b}_m \times \mathbf{u}_m \end{bmatrix}$$

$$\boldsymbol{\tau}_b = \begin{pmatrix} \tau_{b1} & \tau_{b2} & \cdots & \tau_{bm} \end{pmatrix}$$

$$\mathbf{f_e} = \begin{pmatrix} F_x & F_y & F_z & M_x & M_y & M_z \end{pmatrix}$$

here, τ_{bi} is the tension in cable *i* at cable end-point B_i. $\tau_{\min}$ and $\tau_{\max}$ are the minimal and maximal admissible values of cable tensions. $\mathbf{f_e}$ is the wrench applied by the cables on the mobile platform and $\mathbf{W}$ is the so-called wrench matrix.

B. Dynamic Modeling

Let us consider the CDPR driven by m cables shown in Fig. 4. The origin of the frame attached to the mobile platform is O_p. The center of mass of the mobile platform is

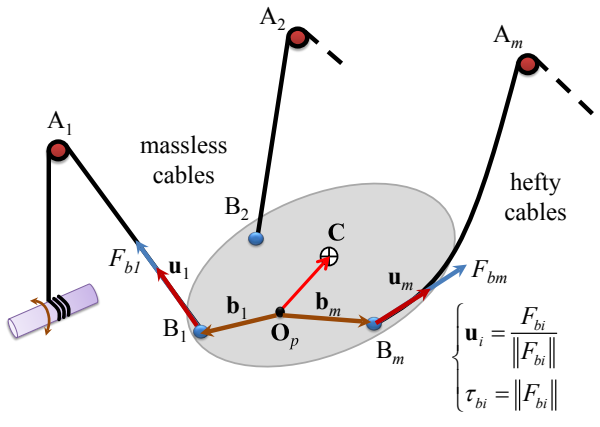

Fig. 4: Sketch of a general $m-$cable CDPR

C. The coordinates of C in frame $\{O_p\}$ are $(x_c \;\; y_c \;\; z_c)$. We consider that the mobile platform moves with acceleration $\mathbf{a}_p$, angular velocity $\boldsymbol{\omega}$ and angular acceleration $\boldsymbol{\alpha}$. Here, the dynamics of the cables and the dynamics of the systems that drive the cable exit points are neglected.

One can derive the equation of motions of the mobile platform as follows:

$$\begin{bmatrix} F \\ M_p \end{bmatrix} + \begin{bmatrix} m_p\, G \\ \mathbf{d} \times m_p\, G \end{bmatrix} = \mathbf{W}\, \boldsymbol{\tau}_b \tag{3}$$

where F and M_p are the inertia force and moment acting on the payload, m_p is the total mass of the mobile platform. $\mathbf{W}$ and $\boldsymbol{\tau}_b$ are defined in (1), $G = (0 \;\; 0 \;\; g)$ with $g = 9.81 m/s^2$, and $\mathbf{d} = \mathbf{R} \cdot \overrightarrow{O_p C}$ where $\mathbf{R}$ is the rotation matrix from the global frame to the mobile platform frame.

It can be seen that (because the center of mass is distinct from O_p):

$$F = m_p\, [\mathbf{a}_p + \boldsymbol{\alpha} \times \mathbf{d} + \boldsymbol{\omega} \times (\boldsymbol{\omega} \times \mathbf{d})] \tag{4}$$

$$M_p = m_p\, \mathbf{d} \times \mathbf{a}_p + \mathbf{I}_p\, \boldsymbol{\alpha} + \boldsymbol{\omega} \times (\mathbf{I}_p\, \boldsymbol{\omega}) \tag{5}$$

where $\mathbf{I}_p$ is the moment of inertia about the reference point O_p of the mobile platform expressed in the global frame:

$$\mathbf{I}_p = \mathbf{R}\, \mathbf{I}_c\, \mathbf{R}^T + m_p\, \left[\left(\mathbf{d}^T\, \mathbf{d} \right) \cdot \mathbf{1}_{3\times 3} - \mathbf{d}\, \mathbf{d}^T \right] \tag{6}$$

Here, $\mathbf{I}_c$ is the polar moment of inertia (or matrix of inertia about the center of mass) of the mobile platform and $\mathbf{1}_{3\times 3}$ is the identity matrix.

IV. CDPR RECONFIGURATION SOLUTION

A. Reconfigurability general concept

In our view, *the reconfigurability of a cable-driven parallel robot is the capability of changing its cable layout to increase the robot flexibility and obtain better performances under certain constraints*. It can be formulated as the following *nonlinear constrained optimization* problem:

"Finding a set of reconfiguration parameters $\mathbf{r}$ which minimizes several performance criteria $\mathbf{f}(\mathbf{r}) = (f_1(\mathbf{r}), f_2(\mathbf{r}), ...)$:

$$\mathbf{r}_{opt} = \min\{\mathbf{f}(r_1, r_2, .., r_p)\} \tag{7}$$

subjects to

$$\mathbf{r_l} \leq \mathbf{r} \leq \mathbf{r_u}$$
$$\mathbf{r} \in \mathbf{C}_r$$

where $\mathbf{r_l}$ and $\mathbf{r_u}$ are the lower and upper bounds on the reconfiguration parameters $\mathbf{r}$. Each criterion f_i is computed with respects to one or several platform poses. $\mathbf{C}_r$ is the set of reconfiguration parameters that satisfy all nonlinear constraints including geometric constraints and wrench feasibility constraints."

In this general problem, there are two types of constraints. The first ones are *geometric constraints* which are the limitations on Cartesian workspace and orientation workspace of the CDPR. Satisfying these constraints means that the CDPR pose at hand is collision free. The second type are *tension based constraints* which *involve the dynamic modeling of the mobile platform* to compute the cable tensions of the CDPR.

In this paper, the considered objective functions to be optimized are cable tensions based performance indices. To ensure the conditions of continuity and differentiability of these criteria, the method in [21] is used to solve the tension distribution of the CDPR.

In order to reduce the complexity of this general optimization problem, we divide it into sub-optimization problems and solve them separately using readily available optimization tools.

B. Desired CDPR performances

In practice, for a certain task, expected working space of a CDPR with desired performances should be defined beforehand as a set of:

- positions in Cartesian space
- orientations
- velocities
- accelerations
- wrenches

which verifies the collision-free and wrench feasible conditions.

The nonlinear constraints corresponding to $\mathbf{r} \in \mathbf{C}_r$ are defined by these desired performances.

C. Sub-optimization problems

1) Determining the bounds on the reconfiguration parameters: The goal of this step is to find lower bounds and upper bounds of the reconfiguration parameters by solving the following optimization problems:

$$\mathbf{r}_{\min} = \min\{\mathbf{r}\} \quad , \; \mathbf{r}_{\max} = \max\{\mathbf{r}\} \tag{8}$$

subject to:

$$\mathbf{r} \in \mathbf{C}_r$$

This step is important since it eliminates the geometric constraints and tension based constraints, thus enabling the use of standard gradient-based optimization tools to solve the general problem (7) more effectively.

The method to solve this problem will be discussed later in more detail in Section VI.

2) Box-constrained optimization problem: Let us assume that the bounds on the reconfiguration parameters are found. Thereby, the general optimization problem (7) is transformed into a box-constrained optimization problem which is much simpler to solve:

$$\mathbf{r}_{opt} = \min\{\mathbf{f}(r_1, r_2, ..., r_p) \mid \mathbf{r} \in \mathbf{B}_r\} \tag{9}$$

where

$$\mathbf{B}_r = \{\mathbf{r} \mid \mathbf{r}_{\min} \leq \mathbf{r} \leq \mathbf{r}_{\max}\} \tag{10}$$

D. Reconfiguration strategy

1) Offline reconfiguration: The aim of offline reconfiguration is to find a set of reconfiguration parameters (locally) optimal with respect to a performance index over the assigned workspace and for given required performances. Let us take an example. Assume that one want the CDPR to reach any pose in a given workspace at any acceleration in a given

range, while keeping the cable tensions within prescribed limits. Offline reconfiguration can consist in finding "the best" locations for the cable exit points allowing the CDPR to do so with minimal power consumption.

To optimize the performance index with respect to the whole workspace, we discretize the latter into a finite set of N equilibrium poses. This procedure is time consuming if there are a lot of discretized points in the finite set to be evaluated. In fact, it is generally satisfactory enough to evaluate the objective function at poses that lie on the boundary of the assigned workspace. Then, the global criterion method [22] is used to find the optimal reconfiguration according to the following steps.

- **Step 1**: Find the optimal configuration $\mathbf{r}_k^*$, $k = 1, 2, ..., N$ for the *k-th* equilibrium pose by solving the box constrained optimization problem:

$$\mathbf{r}_k^* = \min\{f(\mathbf{r}) \mid \mathbf{r} \in \mathbf{B}_r\} \tag{11}$$

  where $\mathbf{B}_r$ is defined in (10) and f is the considered criterion. N is the total number of equilibrium poses considered in the given workspace.
- **Step 2**: Find the optimal configuration $\mathbf{r}_{opt}$ of the following box constrained optimization problem:

$$\text{Minimize } F(\mathbf{r}) = \frac{1}{N}\sum_{k=1}^{N}\left[\frac{f(\mathbf{r}_k^*) - f(\mathbf{r})}{f(\mathbf{r}_k^*)}\right]^2 \tag{12}$$

  subject to $\mathbf{r} \in \mathbf{B}_r$

Offline reconfiguration is in fact a multi-objective optimization problem. A specificity of the problem at hand is that in usual multi-objective optimization there are more than one objective function to be evaluated at a specific pose whereas, in offline reconfiguration, there is only one objective function to be evaluated at many different poses. Furthermore, the priority of evaluating the objective function at every pose in offline reconfiguration can be treated equally which eliminates the difficulty of choosing suitable priority factors for each objective function as in the usual case of multi-objective optimization.

2) Online reconfiguration: In online reconfiguration, we aim to find "the best" CDPR reconfigurations along a given trajectory. The locations of the cable exit points are updated at each sample time in such a way that minimizes a certain performance index.

Because of the real-time constraint, the online reconfiguration should be treated as a single-objective optimization problem. At each sample time, we aim at solving the optimization problem within a few iterations. The number of iterations will be limited by the total time consumption (normally, we could only allow 1, 2 or 3 iterations).

In online reconfiguration, the box constrained optimization problem (9) is defined as follows: At the $s-th$ sample time, find the new values of the reconfiguration parameters

$$\mathbf{r}_{opt}^{(s)} = \min\{\mathbf{f}(r_1, r_2, ..., r_p) \mid \mathbf{r} \in \mathbf{B}_\triangle\} \tag{13}$$

where

$$\mathbf{B}_\triangle = \{\mathbf{r} \mid \mathbf{r}_{opt}^{(s-1)} - \triangle_r \leq \mathbf{r} \leq \mathbf{r}_{opt}^{(s-1)} + \triangle_r\} \tag{14}$$

which also satisfies

$$\mathbf{B}_\triangle \subset \mathbf{B}_r \tag{15}$$

$\triangle_r$ is the maximum step size of the reconfiguration parameters allowed at each sample time.

One can initialize the starting point as the optimal solution found from offline reconfiguration with respect to the same performance index since it reduces the probability of converging to a poor local minimum.

In online reconfiguration mode, two issues must be addressed carefully. Firstly, at each sample time, the new reconfiguration parameters $\mathbf{r}_{opt}^{(s)}$ must not exceed a certain value because of the limitations of the actuators that drive the cable exit points and the cable lengths:

$$\mid r_{iopt}^{(s)} - r_{iopt}^{(s-1)} \mid \leq \triangle_r,\ i = \overline{1, p} \tag{16}$$

Secondly, the movement of the cable exit points and the changes of the cable lengths are coupled together. Because of these issues, the constraint (14) is added in order to maintain the synchronization in driving the cable exit points A_i and the cable lengths in the control system.

E. Cable tension based performance indices

Let us consider a CDPR driven by m cables in a configuration defined by $\mathbf{r}$. At an equilibrium pose of the mobile platform, by solving the tension distribution problem, we achieve desired cable tensions $\tau_i,\ i = 1, 2, ..., m$.

1) Sum of the cable tensions: In **offline reconfiguration**, we choose the sum of the cable tensions as the objective function:

$$f(\mathbf{r}) = \sum_{i=1}^{m} \tau_i(\mathbf{r}) \tag{17}$$

This index relates directly to the power consumption of the CDPR. In case of the proposed *suspended CDPR architecture* (Fig. 3), minimizing this performance index gives us the optimal solution which coincides with the upper bounds on the reconfiguration parameters (an illustrating example is given in Section V). The solution are found using Matlab optimization toolbox or NLopt package [23].

2) Energy consumption: In **online reconfiguration**, we compute the minimal power consumption that is needed to move the mobile platform along a given trajectory, neglecting friction between cables and pulleys or drums and between the mobile bases and the overhead bridge cranes (thus, also neglecting the energy needed to move the cable exit points):

$$E_{on}^{(s)} = \sum_{i=1}^{m} \tau_i^{(s)} . \triangle l_i^{(s)} \tag{18}$$

where $\tau_i^{(s)}$ is the tension of the *i-th* cable (assuming that $\tau_i^{(s)} = const$ during the *s-th* sample time period) and $\triangle l_i^{(s)}$ is the incremental change of the *i-th* cable length.

To verify the results, the total energy consumption along a given trajectory of the mobile platform is computed as

$$E_{total} = \sum_{s=1}^{N_s - 1} E_{on}^{(s)} \tag{19}$$

where N_s is the number of discrete via-points.

V. ILLUSTRATION EXAMPLES

Let us consider a situation where several CDPR are working in a workshop. Each CDPR has to position a heavy platform in several areas which are shown in Fig. 5. In this situation, at each working cell, the positions of the two cranes are fixed. Support beams are used to sustain the horizontal forces created by the cable tensions that tend to bring the two cranes together. The distance between the two cranes is constant and calculated with respect to the size of the working cell. It means that the number of active actuators which reconfigure the positions of the cable exit points is 4 (the 8 cable exit points are moved by pairs). After finishing the workload in an area, the CDPR moves to the next area.

Assume that the CDPR is operating in a given working cell. The size of the CDPR is $22m \times 14m \times 6.4m$ $(l \times w \times h)$. The distance between the two cable exit points within a pair mounted on an overhead bridge crane is $2m$. The mobile platform is a cube of size length $2m$ and weighting $2000kg$. Its center of mass C coincides with the origin of the local frame O_p (which means $d = \overrightarrow{O_pC} = 0$). The characteristics of the steel cables driving the mobile platform are:

- Young modulus $E = 150e+09$ (Pa)
- Cross-section area $A_0 = 4.3937e-05$ (m^2)
- Self-weight $w = 3.3955$ (N/m)

The desired performances of the CDPR are given as:

$$\begin{aligned} m_p &= 2000 \ \ (kg) \\ -4 &\le x_p \le 4 \ \ (m) \\ -5 &\le y_p \le 3 \ \ (m) \\ 0 &\le z_p \le 2.5 \ \ (m) \\ \theta_x &= const = 0 \ \ (deg) \\ -5 &\le \theta_y \le 0 \ \ (deg) \\ 0 &\le \theta_z \le 70 \ \ (deg) \\ -0.7 &\le a_{x,y,z} \le 0.7 \ \ (m/s^2) \\ -0.7 &\le \alpha_{x,y,z} \le 0.7 \ \ (rad/s^2) \\ 100 &\le \tau \le 3.1e+04 \ \ (N) \end{aligned}$$

The considered discretization in *position*, *orientation*, *accelerations*, and *angular accelerations* results in total of $18 \times 8 \times 8 \times 8 = 9216$ cases to be checked to verify the cable tension constraints and collision constraints.

A. Offline reconfiguration

Fig. 6 shows the results of finding the bounds on the reconfiguration parameters $\mathbf{r} = (r_1, \ r_2, \ r_3, \ r_4)$. The equilibrium poses are selected on the edges of the assigned workspace as also shown in Fig. 6.

The solution of minimizing the sum of cable tensions with respect to the given workspace coincides with the upper bounds on the reconfiguration parameters:

$$\mathbf{r}_{opt} \equiv \mathbf{r}_{\max} = (r_{1\max}, \ r_{2\max}, \ r_{3\max}, \ r_{4\max}) \qquad (20)$$

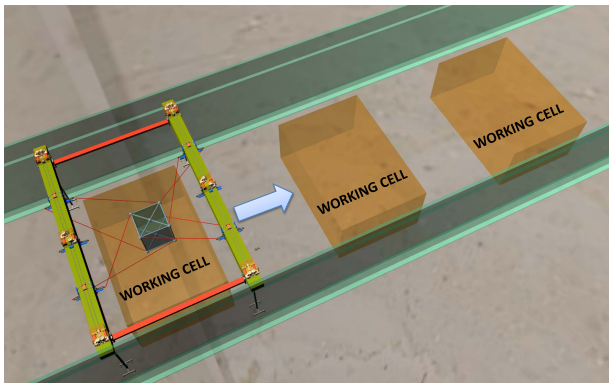

Fig. 5: Example of a scenario in a workshop

B. Online reconfiguration

Currently, we consider online reconfiguration as an optional operation mode since the reliability of the method to solve this problem need to be verified in further studies. In this case, we only present the results assuming that the robot system performs under ideal conditions (e.g. without loss due to friction, perfect synchronization in the control system while updating online the cable lengths and the cable exit point positions). The starting point for online reconfiguration is $\mathbf{r}_{opt}$ given in (20). The objective is to minimize the energy consumption along a trajectory. The maximum step size of the reconfiguration parameters allowed at each iteration is $\triangle_r = 0.005m$.

Smoothed trapezoidal velocity method [24] is used to generate the desired trajectory. The via-points are given in Cartesian workspace and orientation workspace (Euler angle convention) $X = (x \ y \ z, \ \ \theta_x \ \theta_y \ \theta_z) \ \ (m, deg)$:

$$\begin{aligned} X_1 &= (-4.0 \ \ 1.0 \ \ 0.0, \ \ 0 \ \ 0 \ \ 0) \\ X_2 &= (1.0 \ \ -5.0 \ \ 2.0, \ \ 0 \ \ -5 \ \ 30) \\ X_3 &= (0.0 \ \ -2.0 \ \ 2.5, \ \ 0 \ \ -5 \ \ 70) \\ X_4 &= (4.0 \ \ 3.0 \ \ 0.5, \ \ 0 \ \ 0 \ \ 0) \end{aligned}$$

The maximum accelerations and orientation accelerations along the trajectory are $\mathbf{a}_{\max x,y,z} = (0.7 \ \ 0.7 \ \ 0.7) \ \ (m/s^2)$ and $\boldsymbol{\alpha}_{\max x,y,z} = (0.7 \ \ 0.7 \ \ 0.7) \ \ (rad/s^2)$. The time

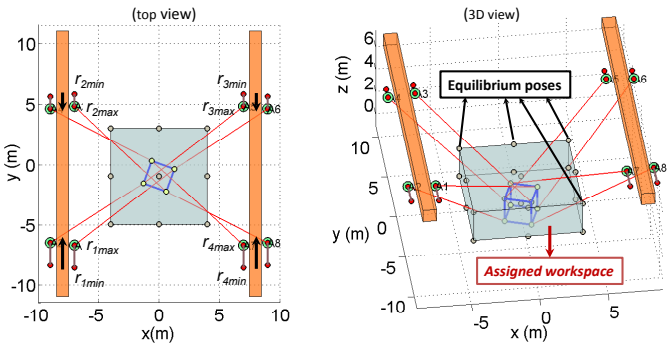

Fig. 6: Bounds on reconfiguration parameters and desired Cartesian workspace

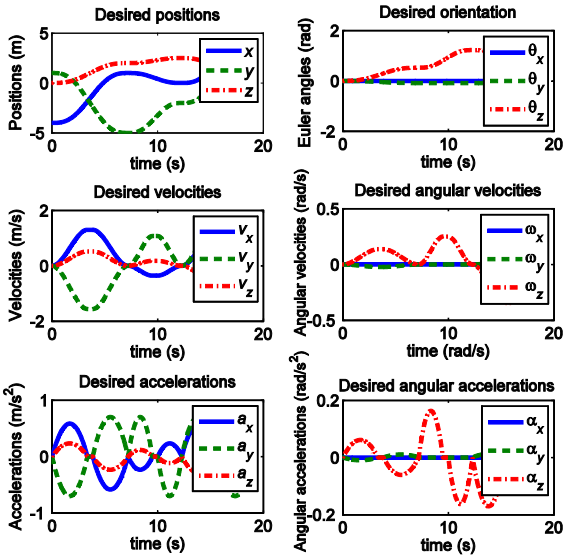

Fig. 7: Desired trajectory

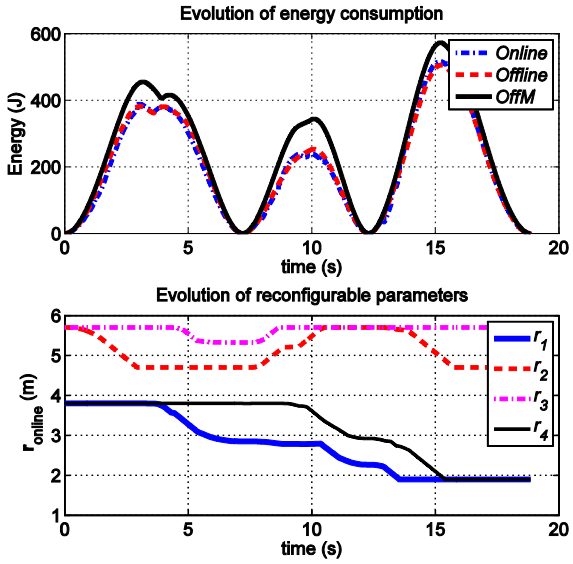

Fig. 8: Results in online reconfiguration

corresponding to the maximum velocity is $t_{v\,\max} = 0.5s$ and the sample time is $dt = 0.01s$. Fig. 7 shows the trajectory generated.

The evolution of the reconfiguration parameters and of the energy consumptions (18) along the trajectory are shown in Fig. 8. E_{OffM} is the minimal energy consumption of the CDPR in configuration $\mathbf{r} = \mathbf{r}_{\min} = (r_{1\,\min},\ r_{2\,\min},\ r_{3\,\min},\ r_{4\,\min})$, $E_{Offline}$ is the minimal energy consumption of the CDPR in configuration $\mathbf{r}_{opt}$ and E_{Online} is the minimal energy consumption for reconfiguration parameters updated online along the trajectory. The total energy consumption (19) in the three cases are computed as:

$$E_{\sum OffM} = 4.5556e+05 \quad (J)$$
$$E_{\sum Offline} = 3.8618e+05 \quad (J)$$
$$E_{\sum Online} = 3.7955e+05 \quad (J)$$

The energy saving rate between offline configuration at $\mathbf{r}_{opt}$ and $\mathbf{r}_{\min}$ is 15.23%. When switching to online reconfiguration, the energy saving rate in this case is 1.7187%. These results show that offline reconfiguration provides a good solution in term of minimizing energy consumption. Under the ideal conditions considered in this paper (no friction, etc.), online reconfiguration mode also reduces the total energy consumption of the CDPR but only slightly compared to offline mode. Note that the optimization tool LBFGS [25] in the nonlinear optimization package [23] was used to solve the boxed constrained optimization problems (9) - (10) in offline and online reconfiguration modes since this method is fast and provides stable results.

VI. REMARK ON THE METHODOLOGY

In our study, we developed a heuristic method to speed up the computation of the upper bounds on the reconfiguration parameters in problem (8) which takes advantage of the particular characteristics of the reconfigurable CDPR family considered in the paper. We may clarify this point as follows.

First of all, let us emphasize two points:

- The cable exit points that reconfigure the CDPR structure are constrained to move along the overhead bridge cranes, i.e., along only one direction
- The considered CDPR are suspended (all cable exit points are located above the mobile platform)

Hence, by minimizing the sum of the cable tensions, the cable exit points will tend to move to the positions where the cables are as vertical as possible while balancing the mobile platform weight. This behavior results in the fact that the optimal solution found in offline reconfiguration coincides with the upper bounds on the reconfiguration parameters as shown in Fig. 6.

Knowing that fact beforehand, we solve the problem (8) as follows. The priority of this step becomes finding the solution that gives the best results in minimizing the sum of cable tensions, which also means finding the maximum value of the upper bound vector $\mathbf{r}_{\max}$. Fig. 9a shows the optimal solution. Whereas, Fig. 9b shows a solution for the upper bound vector where we try to increase the value of $r_{2\,\max}$ which results in reducing the values of $r_{3\,\max}$ substantially. It is due to the fact that, in order to satisfy the conditions of wrench feasibility and the geometric constraints, the span

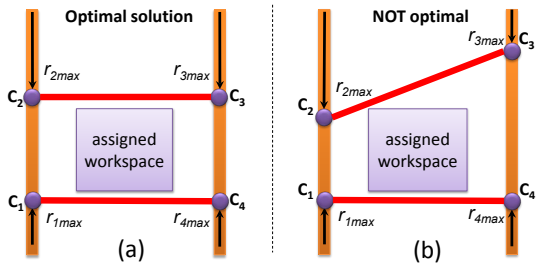

Fig. 9: Solution for the upper bounds on the reconfiguration parameters

of cable exit points (the polygon $C_1C_2C_3C_4$) should cover the assigned workspace (the rectangle box). The changes in $r_{2\max}$ and $r_{3\max}$ shown in Fig. 9b result in increasing the value of the sum of cable tensions. Therefore, updating the values of the pairs of reconfiguration parameters (r_1, r_4) and (r_2, r_3) along the directions that keep the line C_1C_4 and C_2C_3 orthogonal to the overhead bridge cranes should lead us to the optimal solution. This heuristic helps a lot to reduce the computation time needed to solve the sub-optimization problem (8).

In fact, in the examples shown in Section V, while solving problem (8), we set the maximum displacement of updating the reconfiguration values in each iteration to $dr = 0.1\,m$. The time needed to find only the upper bound vector $\mathbf{r}_{\max}$ is around $2\,min$ (which is quite fast). However, the total time needed to find the lower bound vector $\mathbf{r}_{\min}$ (including checking all the constraints at all discretized poses) is around $40 - 50\,min$. In online reconfiguration, the time estimated for each iteration is around $30 - 40\,ms$. We use MATLAB on a PC with core $i7 - 2.7GHz$ to run the simulations.

CONCLUSIONS

We have presented in this paper a solution using large-dimension reconfigurable suspended CDPR to replace conventional methods of handling heavy payloads across a wide workspace. The introduced reconfigurable CDPR family can be adapted in various environments and is expected to have great potential.

Critical issues in solving the reconfiguration of this CDPR have been discussed. By transforming the general complex problem into more simple sub-optimization problems, we can take advantage of readily available tools to derive an optimal solution. In situations where there is no reliable method to handle difficult issues in online reconfiguration, offline reconfiguration offers a more reliable choice to the end-users. Furthermore, the presented method to determine offline reconfigurations can be applied to specific cases such as finding the optimal solution for a given trajectory.

It is also worth noting that, besides the two presented performance indices, there are important criteria that determine the quality of a CDPR such as the stiffness at the mobile platform. They can be implemented within the framework of the procedure proposed in this paper is part of our future work.

ACKNOWLEDGMENT

The research leading to these results has received funding from the European Community's Seventh Framework Programme under grant agreement No. NMP2-SL-2011-285404 (CABLEBOT).

REFERENCES

[1] J. Albus, R. Bostelman, and N. Dagalakis, "*The NIST robocrane*," *Journal of Robotic Systems*, vol. 10, no. 5, pp. 709–724, 1993.

[2] A. B. Alp and S. K. Agrawal, "*Cable suspended robots: design, planning and control*," *Proceedings of IEEE International Conference on Robotics and Automation,ICRA 2002*, pp. 4275–4280, 2002.

[3] S.-R. Oh and S. K. Agrawal, "*The feasible workspace analysis of a set point control for a cable-suspended robot with input constraints and disturbances*," *IEEE Transactions on Control Systems Technology*, vol. 14, no. 4, pp. 735–742, 2006.

[4] S. Bouchard, C. Gosselin, "*Kinematic sensitivity of a very large cable-driven parallel mechanism*," *ASME International Design Engineering Technical Conferences*, 2006.

[5] M. Hassan, A. Khajepour, "*Analysis of Large-Workspace Cable-Actuated Manipulator For Warehousing Applications*," *ASME International Design Engineering Technical Conference*, 2009.

[6] B. Duan, Y. Qiu, F. Zhang, B. Zi, "*On design and experiment of the feed cable-suspended structure for super antenna*," *Mechatronics*, vol. 19, pp. 503–509, 2009.

[7] N. Riehl, M. Gouttefarde, C. Baradat, F. Pierrot, "*On the determination of cable characteristics for large dimension cable-driven parallel mechanisms*," *IEEE International Conference on Robotics and Automation, ICRA 2010*, pp. 4709–4714, 2010.

[8] R. Yao, X. Tang, J. Wang, P. Huang, "*Dimensional Optimization Design of the Four-Cable-Driven Parallel Manipulator in FAST*," *IEEE/ASME Transaction on Mechatronics*, vol. 15, no. 6, pp. 932–941, 2010.

[9] H. Li, X. Zhang, R. Yao, J. Sun, G. Pan and W. Zhu, "*Optimal Force Distribution based on slack rope model in the incompletely constrained cable-driven parallel mechanism of FAST telescope*," *Cable-Driven Parallel Robots, Mechanism and Machine Science, Springer*, vol. 2, pp. 87–102, 2013.

[10] R. Yao, H. Li, X. Zhang, "*A Modeling Method of the Cable Driven Parallel Manipulator for FAST*," *Cable-Driven Parallel Robots, Mechanism and Machine Science, Springer*, vol. 12, pp. 423–436, 2013.

[11] N. Riehl, M. Gouttefarde, S. Krut, C. Baradat and F. Pierrot, "*Effects of non-negligible cable mass on the static behavior of large workspace cable-driven parallel mechanisms*," *IEEE International Conference on Robotics and Automation*, pp. 2193–2198, 2009.

[12] E. Ottaviano, G. Castelli, "*A Study on the Effects of Cable Mass and Elasticity in Cable-Based Parallel Manipulator*," *Proc. f the18th CISM-IFToMM Symp. On Robot Design, Dynamics and Control, Springer Ed. Udine*, pp. 149–156, 2010.

[13] D. Q. Nguyen, M. Gouttefarde, O. Company and F. Pierrot, "*On the simplifications of cable model in static analysis of large-dimension cable-driven parallel robots*," *IEEE International Conference on Intelligent Robots and Systems (IROS)*, pp. 928–934, 2013.

[14] M. Gouttefarde, J. Collard, N. Riehl, C. Baradat, "*Simplified static analysis of large-dimension parallel cable-driven robots*," *IEEE International Conference on Robotics and Automation*, pp. 2299–2305, 2012.

[15] J.-P. Merlet, D. Daney, "*A portable, modular parallel wire crane for rescue operations*," *2010 IEEE International Conference on Robotics and Automation (ICRA)*, pp. 2834 – 2839, May 2010.

[16] J. Lamaury, M. Gouttefarde, "*Control of a Large Redundantly Actuated Cable-Suspended Parallel Robots*," *Proceedings of the IEEE International Conference on Robotics and Automation (ICRA)*, 2013.

[17] MHS, "*Aerial Multi-axis Platform (AMP)*," *http://www.mhs-llc.com/custom-multi-axis-positioning-material-handling-system*.

[18] G. Rosati, D. Zanotto, S. K. Agrawal, "*On the Design of Adaptive Cable-Driven Systems*," *Journal of Mechanisms and Robotics, ASME*, vol. 3, May 2011.

[19] X. Zhou, C.P. Tang, and V. Krovi, "*Analysis Framework for cooperating Mobile Cable Robots*," *IEEE International Conference on Robotics and Automation*, pp. 3128–3133, May 2012.

[20] X. Zhou, C.P. Tang, and V. Krovi, "*Cooperating Mobile Cable Robots: Screw Theoretic Analysis*," *Lecture Notes in Electrical Engineering, Springer Berlin Heidelberg*, vol. 57, pp. 109–123, May 2013.

[21] J. Lamaury, M. Gouttefarde, "*A tension distribution method with improved computational efficiency*," *Cable-Driven Parallel Robots, Mechanisms and Machine Science, Springer*, vol. 12, pp. 71–85, 2013.

[22] S. S. Rao, *Engineering Optimization: Theory and Practice*. John Wiley & Sons, 2009.

[23] S. G. Johnson, "*The NLopt nonlinear-optimization package*," *http://ab-initio.mit.edu/nlopt*.

[24] W. Khalil, Étienne Dombre, *Modeling, Identification And Control of Robots*. Hermes Penton, 2002.

[25] L. Luksan, "*Low-storage BFGS algorithm*," *http://www.uivt.cas.cz/ luksan/subroutines.html*.